Slip-History of the Vincent Thrust: Role of Denudation During Shallow Subduction

Marty Grove and Oscar M. Lovera

Department of Earth & Space Sciences, University of California, Los Angeles

$^{40}Ar/^{39}Ar$ age and ^{39}Ar kinetic studies performed with K-feldspars sampled from above the Vincent Thrust (VT) allow reconstruction of its slip history during Late Cretaceous-Early Tertiary shallow subduction. Variational methods were applied to the multiple diffusion domain model to produce best fit thermal histories. The K-feldspar T-t results indicate that a temperature difference of ~150°C was maintained from >60 Ma to <55 Ma between positions that are presently at nearly the same elevation and are located 5 and 15 km west of the VT. Using a geothermal gradient and dip angle estimated from geologic constraints, simple numerical heat-flow models were used to determine the slip velocity and relative vertical separation of the samples during thrusting by requiring calculated T-t results to fit the K-feldspar thermal histories. For models in which cooling was due solely to subduction of colder rocks (hanging wall stationary), solutions most compatible with the K-feldspar results were yielded by underthrusting rates of ~1.4 cm/yr. and a vertical separation during the Late Cretaceous/Early Tertiary of 8.5 km. Allowing denudation of the hanging wall during thrusting (footwall stationary) provides somewhat more satisfactory fits to the data. For these models, ~0.2-0.4 cm/yr. displacement occurs along the VT from 65 Ma to 50 Ma along a fault plane inclined at 15°. Because only net vertical displacement can be constrained by K-feldspar data, our calculated slip rate is only a relative value that is inversely proportional to the dip angle at the time of thrusting.

1. INTRODUCTION

Knowledge of the slip history of subduction-related thrust faults is fundamental to understanding convergent margin evolution. Since tectonic movements modify the distribution of thermal energy within the crust, combined thermochronology and numerical heat-flow analysis offer a powerful means of evaluating tectonic models. Within subduction complexes, attention has generally been focused upon constraining thermal histories of accreted materials. In this contribution, we employ thermochronologic results from the Vincent Thrust (VT) of southern California together with simple numerical heat-flow calculations to demonstrate that knowledge of the temperature-time evolution above subduction complexes can also provide important insights. Our methods [Lovera et al., 1989] feature thermochronology based upon $^{40}Ar/^{39}Ar$ age and ^{39}Ar kinetic experiments performed with K-feldspar that are capable of constraining temperature-time histories of processes active within the middle crust (~400-150°C).

Subduction: Top to Bottom
Geophysical Monograph 96

2. GEOLOGIC OVERVIEW

The VT within the eastern San Gabriel Mountains (Fig. 1) juxtaposed a Cretaceous magmatic arc and older crystalline rocks of the San Gabriel terrane over a subduction assemblage (the Pelona Schist) during the Late Cretaceous-Early Tertiary. The Pelona Schist and its regional equivalents (Fig. 1) consist of metamorphosed flysch, mafic, and minor ultramafic assemblages recrystallized under amphibolite, epidote amphibolite, greenschist, or rarely epidote blueschist facies conditions [Graham and Powell, 1984; Jacobson and Dawson, 1995]. These rocks are widely believed to have been accreted beneath the VT and related faults during Late Cretaceous-Early Tertiary shallow subduction [Coney and Reynolds, 1977; Graham and England, 1976; Burchfiel and Davis, 1981; Dickinson, 1981]. While Late Tertiary reactivation of this suture was widespread [Jacobson and Dawson, 1995 and references therein], structural, petrologic, and thermochronologic evidence all imply that an unmodified

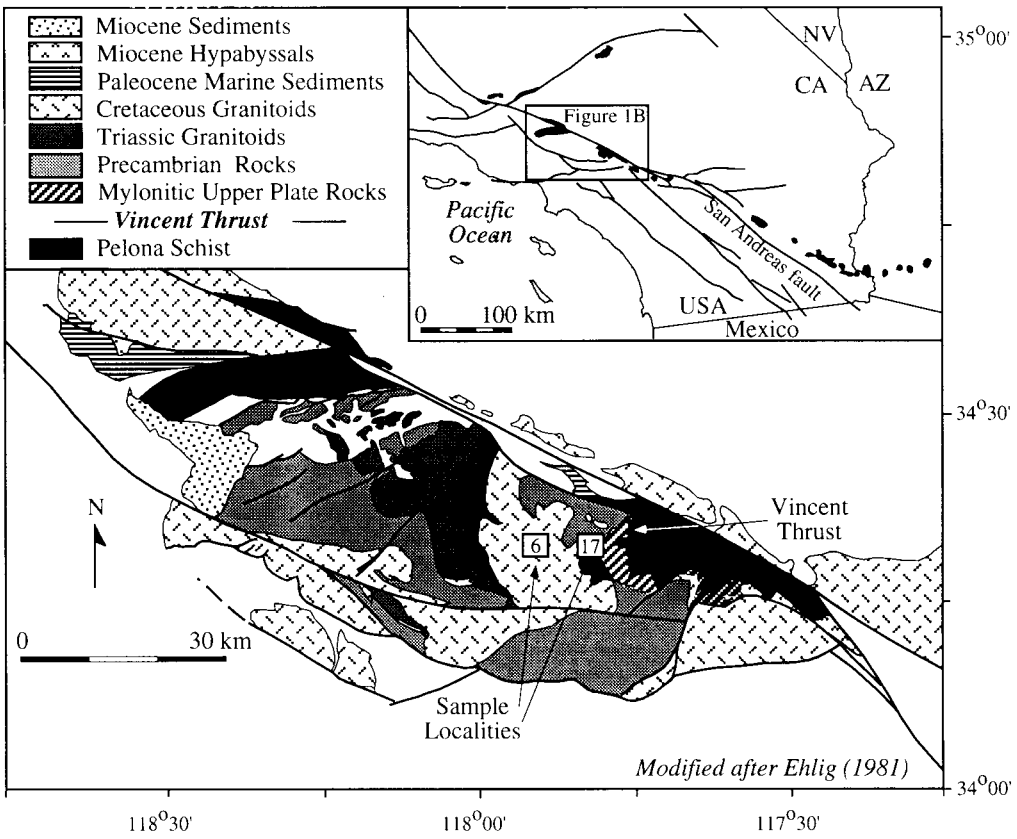

Fig. 1: (A) Regional distribution of Pelona Schist and related rocks in southwestern North America (indicated by black filled regions). Rocks exposed in the San Gabriel mountains (inset) have been displaced ~240 km along the San Andreas fault from their equivalents in SE California. (B) Geologic sketch map of the San Gabriel mountains illustrating the position of the Vincent thrust and samples discussed in the text.

thrust fault contact is preserved across the VT in the northeastern San Gabriel Mountains. Significant reactivation of the VT is seemingly precluded by the pattern of inverted metamorphism beneath the fault and development of isofacial mineral assemblages and concordant fabrics in the underlying schist and mylonitic upper plate rocks at the contact [Ehlig, 1981, Jacobson, 1983, 1995]. Similarity of mica K-Ar cooling ages above and beneath the VT also implies shared histories for the upper and lower plates during the early Tertiary [Jacobson, 1990 and references therein].

3. TESTING TECTONIC MODELS

Previous numerical modeling studies that have sought to explain the inverted metamorphic zonation beneath the VT have offered significantly different estimates of its slip history. Using relatively high estimates for shear heating (125-250MPa @ 3cm/yr = 0.12-0.24 W/m^2), Graham and England [1977] produced models that required displacement of ~90 km accompanied by 0.2 mm/yr erosion to avoid temperature increases unsupported by geologic observations. Peacock [1987] alternatively found that underflow of many hundreds of kilometers of oceanic crust was required to create and preserve the inverted metamorphic gradient across the VT if frictional heating was negligible. Similarly, Dumitru [1991] has invoked refrigeration of the Cretaceous magmatic arc during rapid, shallow-angle Laramide subduction beneath western North America. Note that although denudation of the VT hanging wall was potentially significant [Mahaffie and Dokka, 1986; Dillon, 1986; May and Walker, 1989], no numerical studies of the VT have explicitly considered it.

In the present paper, we discuss results from two K-feldspar samples supplied by A.P. Barth. The specimens were obtained at positions 5 and 15 km west of, and above, the presently exposed trace of the VT (Fig. 1). Both sample localities occur approximately at the same elevation. The

specimens examined consist of homogeneous orthoclase (93-NG-17) and microcline with minor perthite (93-NG-6). Both were obtained from intrusions that are texturally similar to the youngest dated plutons (~80-75 Ma) emplaced into the VT hanging wall prior to thrusting [May and Walker, 1989; Barth et al., 1995]. A sample adjacent to 93-NG-17 has yielded a U-Pb sphene age of 77±2 Ma [Joe Wooden, unpublished data] and a hornblende inverse isochron age of 71±2 Ma [sample 93-NG-13; $^{40}Ar/^{39}Ar$ data tables and plots for this and other samples discussed in the text are available at the following WWW site: http://oro.ess.ucla.edu/argon.html].

4. THERMAL HISTORY RECONSTRUCTION

K-feldspar $^{40}Ar/^{39}Ar$ age and ^{39}Ar kinetic data allow reconstruction of thermal histories of mid-crustal rocks (~150-400°C) through use of the multiple diffusion domain (MDD) model [Lovera et al., 1989]. In this mode', differing intra-sample argon retentivities are assumed to result from a discrete distribution of non-interacting diffusion domains that vary in dimension (r). The form of the Arrhenius plot ($\log(D/r^2)$ vs. 1/T; see Fig. 2b) or its associated $\log(r/r_o)$ plot [Fig. 2c; see Richter et al., 1991] is a function of the parameters that characterize the individual diffusion domains (activation energy (E), frequency factor (D_o), domain size (ρ), and volume fraction (ϕ)). Although the age spectrum (Fig. 2a) also depends upon these parameters, its shape is further modulated by the thermal history.

We have recently incorporated new automated routines [Lovera et al., 1995] that allow thorough analysis of the K-feldspar results. Levenberg-Marquardt variational methods (a generalization of least squares routines to non-linear cases) are used to find the maximum likelihood estimate of the model parameters [Press et al., 1988]. From the ^{39}Ar data, values for E and $\log(D_o/r_o^2)$ are found from a linear, weighted, least-squares fit to the initial, low-temperature $\log(D/r^2)$ values (Fig. 2b). The maximum likelihood estimate of the distribution parameters (ρ, ϕ) is then obtained by applying the variational method. With these values, the Levenberg-Marquardt method is again applied to model the measured $^{40}Ar/^{39}Ar$ age spectrum by varying the coefficients of Chebyshev polynomials used to approximate the thermal history until an acceptable solution is returned. In the present study, we have restricted our solutions to monotonic cooling by constraining the first derivative of the thermal history to be negative. Since uncertainties in age and non-linearity of the diffusion process give rise to multiple solutions (Fig,2d), we use contour plots to indicate the probability distribution of the thermal history.

5. THRUST FAULT MODELS

Simple, two-dimensional, numerical heat-flow models with thrust fault geometry and kinematics have been investigated. Calculations involved finite-difference methods using direct and alternating-direction implicit techniques. Thermal diffusivity was set at an average crustal value $\kappa = 10^{-6}$ m^2/sec. Constant temperature was maintained both at the surface (25°C) and base (1025°C) of the grid while a zero heat flux condition was imposed over the lateral boundaries. Frictional and internal heating (due to radioactive decay and metamorphic reactions) were not considered. Although frictional heating can significantly influence temperature distributions adjacent to the fault [Molnar and England, 1990], our calculations using shear stress values we consider reasonable (~25 MPa; cf. Peacock, 1992) indicate that samples situated more than ~3 km from the fault are only mildly affected by the frictional heating. The effect of frictional heating along the fault can essentially be compensated by an equivalent decrease of the slip rate (i.e., neglecting internal heating could lead to a slight underestimation of the slip rate).

6. DISCUSSION

Combined K-feldspar thermochronology and numerical heat-flow calculations allow us to estimate the displacement history of the VT. Given a geothermal gradient and dip angle, we are able to use the numerical heat-flow models to constrain the slip velocity and relative vertical separation of the samples by requiring the T-t results to agree with the K-feldspar thermal histories. A 25°C/km geothermal gradient and 15° dip angle have been used in all of the numerical heat-flow models. The geothermal gradient can be estimated from available petrologic and thermochronologic data. Assuming ~20 km emplacement depths [Barth, 1990; Barth et al., 1995], closure systematics of Pb in sphene and Ar in hornblende imply both a ~25°C/km geothermal gradient and slow cooling of 93-NG-17 through 600-450°C from >77 Ma to <70 Ma. The original dip of the VT is more uncertain since Neogene doming of the VT due to transpressional deformation resulting from San Andreas-related, strike-slip faulting precludes precise determination of this parameter (Fig. 1). Although the sinuous map pattern of the VT (Fig. 1) indicates that it dips gently at the surface, geologic relationships suggest that the fault rotates to a steeper orientation in the west beneath our samples. To the extent that the VT originally dipped at a shallower angle, this relationship implies that the WNW-trending domal uplift shown in Fig. 1 has exposed progressively deeper rocks moving eastwards toward the VT.

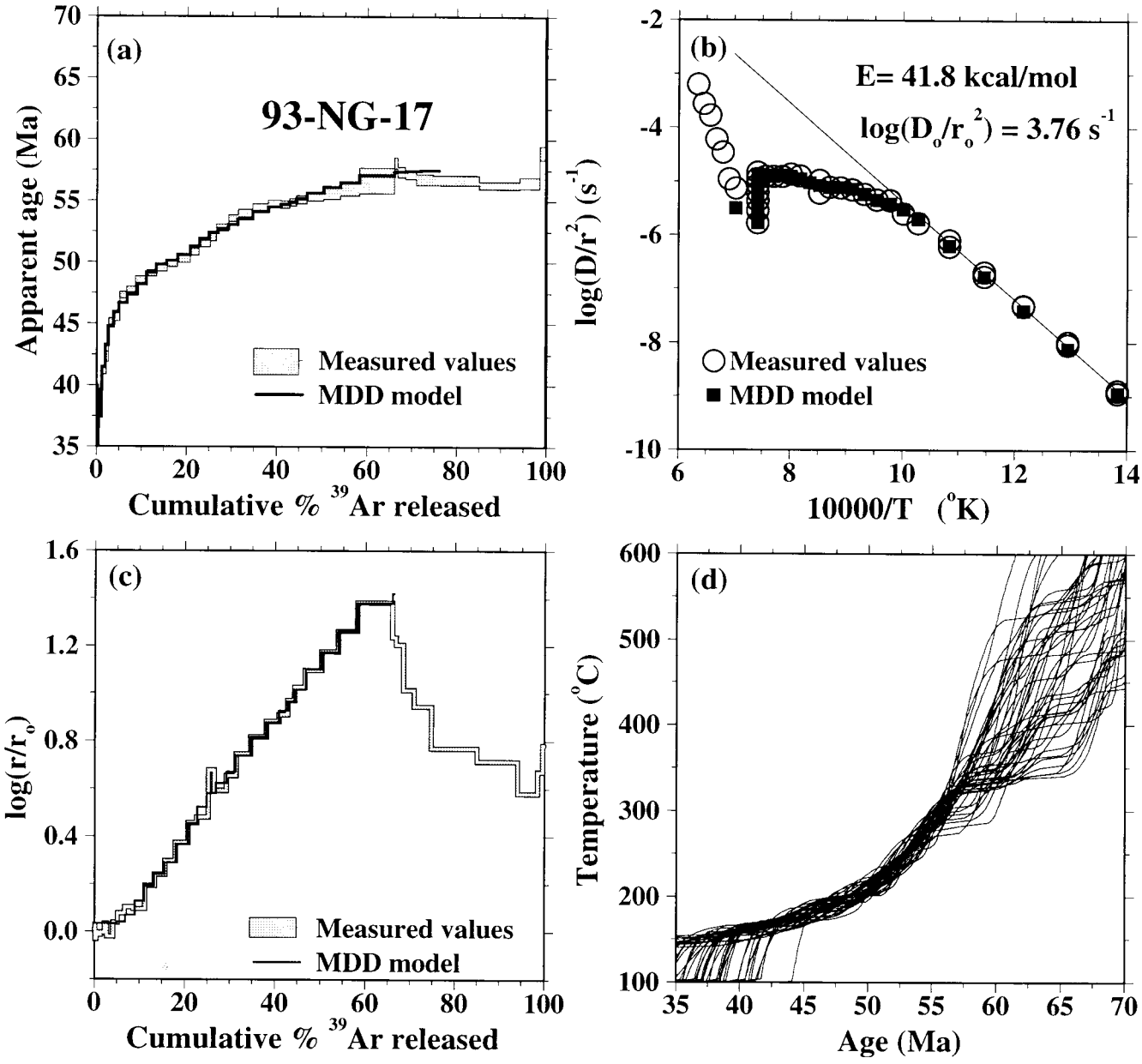

Fig. 2: Thermochronologic constraints from 93-NG-17 K-feldspar. (a) Measured and calculated age spectra; (b) Arrhenius plot calculated from ^{39}Ar loss (circles) and from the MDD model fit (squares). Isothermal duplicates have been performed at low temperatures (<700°C); (c) $\log(r/r_o)$ plot showing values calculated from laboratory data and MDD model fit. Results are modeled only to 1100°C since melting has occurred at higher temperatures. A cross correlation value of 0.99 was obtained between the $\log(r/r_o)$ plot and age spectra (to 1100°C); (d) Calculated thermal histories which fit the measured age spectrum in (a) above. The solid curve in (a) is a representative solution obtained from one of these monotonic cooling curves. The cooling thermal histories are constrained to within ±10°C between 350-150°C. A contour plot of the calculated thermal histories is shown in Fig.4a.

Thermochronologic constraints provided by our samples and by previous studies are most consistent with motion along the VT initiating sometime between ~63-69 Ma and continuing to ~50 Ma. As mentioned above, $^{40}Ar/^{39}Ar$ hornblende and U-Pb sphene for a sample adjacent to 93-NG-17 indicate slow cooling through ~550-450°C from > 77 Ma to < 70 Ma. Amphibole $^{40}Ar/^{39}Ar$ ages of 58-65 Ma from epidote amphibolite mafic schists within the underlying Pelona Schist [Jacobson, 1990] and regional biotite closure at ~65 Ma within higher structural levels in the upper plate [Miller and Morton, 1980] likely constrain the time of initial thrusting. Previous Rb-Sr, K-Ar and $^{40}Ar/^{39}Ar$ results from upper plate mylonites and lower plate micas summarized in [Jacobson, 1990] indicate continued cooling between 60-50 Ma. The initial 5-10% of gas released from both our samples is consistent with slow cooling below 200°C at times later than 50 Ma (Fig. 2d).

Based upon these observations, we have initiated slip at 65 Ma in our numerical models. Isothermal distributions at selected times for two end member cases are shown in Fig. 3a-f. In the first (Model I; Fig. 3a-c), the footwall is maintained stationary while uplift of the hanging wall due to thrusting is balanced by erosion (pure denudation). In the second (Model II; Fig. 3d-f), the hanging wall is fixed (no denudation) while the footwall is subducted. Although we vary the relative vertical separation of the samples in the models to obtain the best agreement with the K-feldspar results, their overall separation is fixed by their present geographic coordinates (10 km; Fig. 1). Because we are most confident in our ability to project surface geology beneath the sample which lies closest to the VT (93-NG-17), we maintain its position at 3.5 km above the fault in both models.

In the following discussion we consider only the solutions to models I and II which produce T-t histories in best agreement with the K-feldspar thermal history results. The results for hanging wall positions indicated in Fig. 3 are shown in Fig. 4a together with contoured T-t histories yielded by K-feldspar thermochronology. Reference to Fig. 4b enables evaluation of T-t conditions for which the K-feldspar thermal history results are able to constrain the numerical models in Fig. 4a. For example, 93-NG-6 provides constraints from 63 to ~55 Ma (Fig. 4b).

The thermal model results shown in Fig. 4a indicate that denudation and cooling of the hanging wall in the manner described by Model I can easily account for the K-feldspar thermal history results. Our best fits are obtained for a relative vertical separation of ~6 km and a net vertical displacement of ~10 km from 65-50 Ma (Fig. 3a-c). Note that the slip rate was increased from ~0.2 to ~0.4 cm/yr between 60-56 Ma to account for the rapid cooling indicated by both samples at this time. Although the model result for 93-NG-6 deviates significantly from the K-feldspar T-t results beyond 55 Ma in Fig. 4a, this portion of the thermal history is constrained only by the first 5% of gas release from the sample (Fig. 4b). Assuming that the fault originally dipped at 15°, the estimated vertical separation of 6 km implies rotation of the VT to a present-day ~50° dip in the subsurface beneath the two samples, possibly due to Neogene doming.

Results from Model II yield somewhat less satisfactory fits to the K-feldspar thermal history results (Fig. 4a-b). Although a closely matched solution is obtained for 93-NG-6 using a subduction rate of 1.5 cm/yr, considerable misfit of 93-NG-17 results (Fig. 4b). More significantly, the best fit to 93-NG-6 requires that the samples be separated vertically by ~8.5 km. This value implies rotation of the VT to a present-day 75° dip in the subsurface beneath the samples. We believe that such a steep inclination of the VT is unsupported by the surface geology. Slip-rates faster than 1.5 cm/yr. require the vertical separation of the samples to exceed the 10 km distance that presently separates them. Alternatively, slower rates of displacement produce steady state temperatures higher than those required to model the K-feldspar thermal history after ~57 Ma.

Although the match to the K-feldspar thermal history results for the case of pure subduction (Model II) is less satisfactory than that obtained for Model I, it appears from Fig. 4a that an improved interpretation would result by considering combined subduction of the lower plate and denudation of the hanging wall. For example, subduction starting at ~65 Ma can account for the slow cooling portion of the thermal histories (>60 Ma and <56 Ma) if the rapid cooling between 60-56 Ma is explained by the superposed effects of subduction plus denudation.

In comparing our results to those obtained in previous studies [Graham and England, 1976; Peacock, 1987], we emphasize that these authors lacked thermochronologic constraints and therefore were concerned only with explaining the formation and preservation of the inverted metamorphic zonation across the VT. Graham and England's preferred model (3 cm/yr displacement for 3 Ma with 0.12 W/m^2 (125 MPa) shear heat source) predicts temperatures that are too high in the VT hanging wall after ~56 Ma to explain the K-feldspar results. Alternatively, Peacock's [1987] model predicts temperatures in the hanging wall that are too low after ~56 Ma.

From the available thermochronology and the simple numerical calculations presented above, we conclude that appreciable (~1 mm/yr.) denudation of the VT hanging wall (particularly between 60-56 Ma; see Model I) likely accompanied modest (<1 cm/yr) underflow of the colder rocks from 65 to <50 Ma. We emphasize that the displacement rates in model I (0.2-0.4 cm/yr) represent

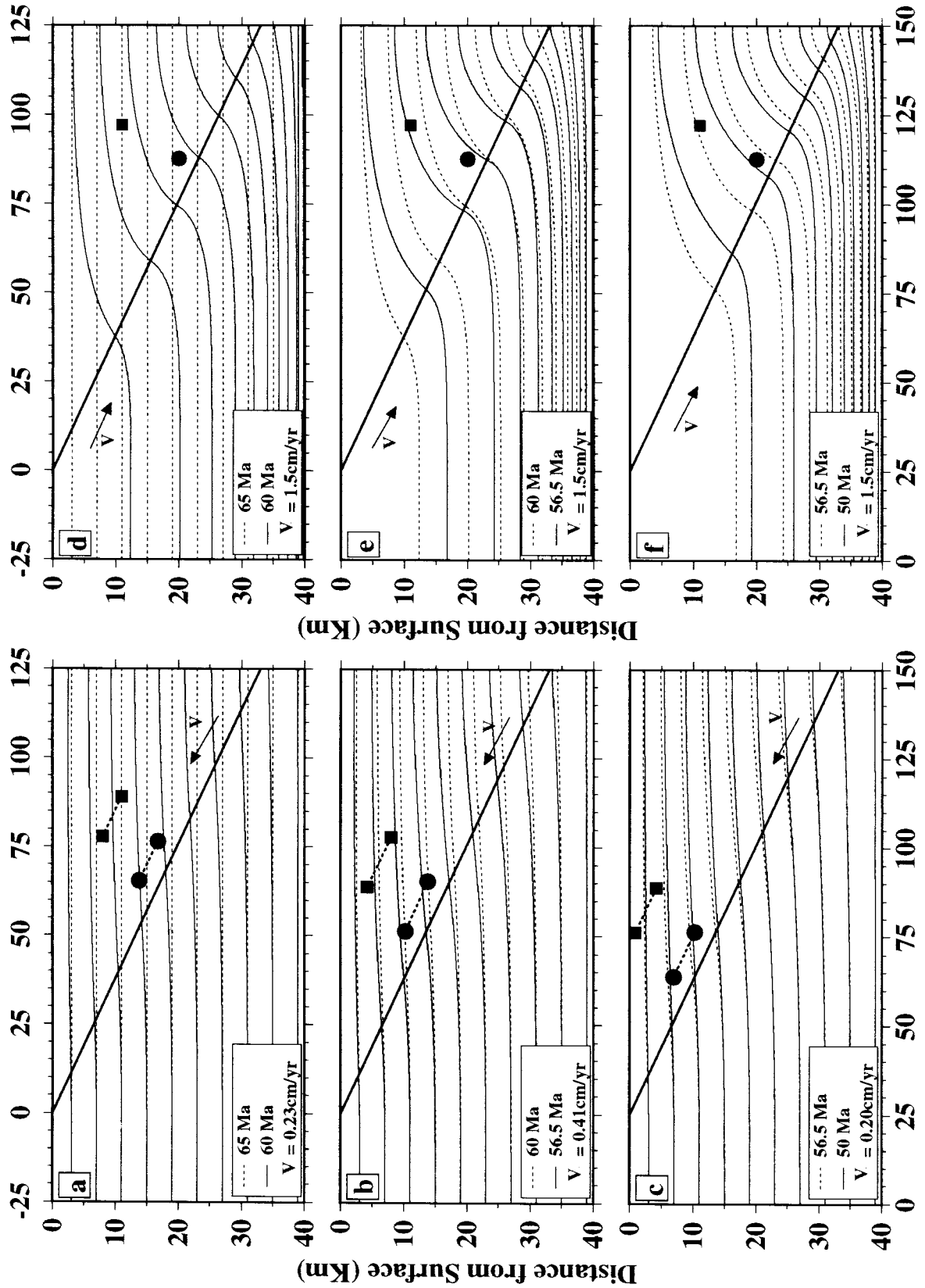

Fig. 3: Isothermal sections produced from the heat-flow calculations. In model I (a-c), the footwall is fixed while the hanging wall is thrust upwards (denudation and erosion balanced at the surface). In model II (d-f), the hanging wall is stationary while the footwall is subducted. The vertical separation maintained between the samples is 6 km and 8.5 km for models I and II respectively. In both models slip is initiated at 65 Ma. Note that the slip velocities employed between each of the indicated times are provided.

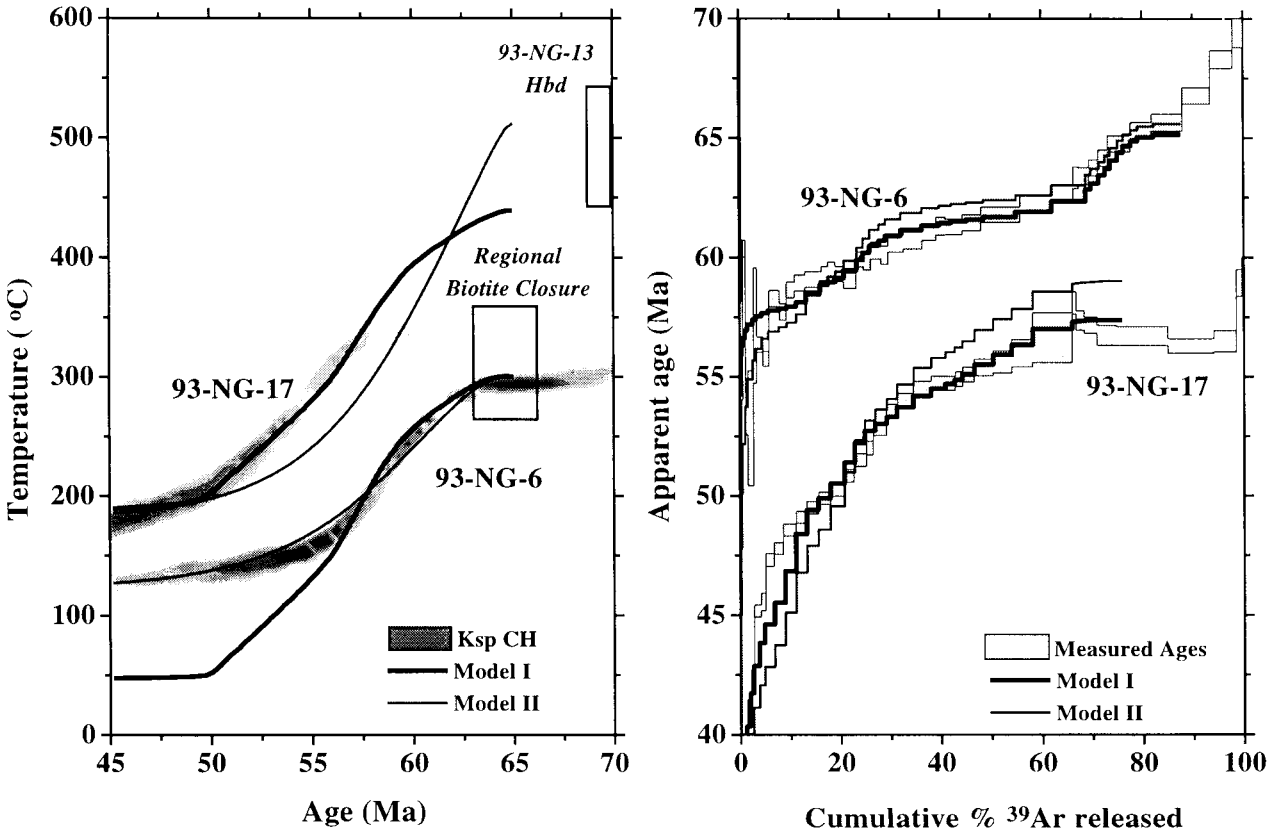

Fig. 4: (a) Thermal evolution of the VT. Thermal histories density contours calculated for 93-NG-17 and 93-NG-6 K-feldspars (45 results each) are represented by shades of gray. The lowest density shown represents a >50% probability that a solution lies within the indicated region.. Open boxes indicate thermochronologic constraints provided by 93-NG-13 hornblende (adjacent to 93-NG-17) and biotite results for the central San Gabriel Mountains (similar to 93-NG-6). Calculated thermal histories from Model I and II for the sample positions indicated in Fig. 3 are shown in bold and light lines respectively. (B) Age spectra calculated from models I and II are compared to the measured K-feldspar age spectra. Note that although Model II yield a satisfactory fit to the measured age spectrum of 93-NG-6, it fails to reproduce that of 93-NG-17 K-feldspar.

relative values that are inversely proportional to the dip angle. If the fault shallowed to become subhorizontal at depth, our model for the slip history of the VT would clearly underestimate the total magnitude of displacement. Similarly, although the thermochronologic data preclude significant underflow of colder rocks beneath the VT hanging wall prior to ~65 Ma, earlier motion along a subhorizontal fault that juxtaposed rocks of equivalent temperature cannot be ruled out.

Acknowledgments. The samples examined in this study were provided by A.P. Barth (funding by the National Geographic Society). We particularly thank C.E. Manning, T.M. Harrison, A.P. Barth, B. Idelman, and A.C. Warnock for providing constructive reviews. Aspects of this research were supported by grants from NSF (Lovera) and DOE (Harrison).

REFERENCES

Barth, A.P., Mid-crustal emplacement of Mesozoic plutons, San Gabriel Mountains, California, and implications for the geologic history of the San Gabriel Terrane, *in The nature and origin of Cordilleran magmatism,* edited by J.L. Anderson, *Geol. Sci. Am.Mem. 174*, 33-45, 1990.

Barth, A.P., Wooden, J.L., Tosdal, R.M., Morrison, J., Crustal contamination in the petrogenesis of a calc-alkalic rock series: Josephine Mountain intrusion, California, , *Geol. Sci. Am. Bull., 107*, 201-212, 1995.

Burchfiel, B.C., and G.A. Davis, Mojave Desert and environs, *in The Geotectonic Developement of California, Rubey Vol. I,* edited by W.G. Ernst, pp. 217-252, Prentice-Hall, Englewood Cliffs, N.J., 1981.

Coney P.J., and S.J. Reynolds, Cordilleran Benioff Zones, *Nature, 270*, 403-406, 1977

Dickinson, W.R., Plate tectonics and the continental margin of California, *in The Geotectonic Developement of California, Rubey Vol. I*, edited by W.G. Ernst, pp. 1-28, Prentice-Hall, Englewood Cliffs, N.J., 1981.

Dillon, J.T., Timing of thrusting and metamorphism along the Vincent-Chocolate Mountain thrust system, southern California, *Geol. Sci. Am. Abstr. Programs, 18*, 101, 1986.

Dumitru, T.A., Effects of subduction parameters on geothermal gradients in foreacs, with an application to Franciscan subduction in California, *JGR, 96* (B1), 621-641, 1991.

Ehlig, P.L., Origin and tectonic history of the basement terrane of the San Gabriel Mountains, central Transverse Ranges, *in The Geotectonic Developement of California, Rubey Vol. I*, edited by W.G. Ernst, pp. 253-283, Prentice-Hall, Englewood Cliffs, N.J., 1981.

Graham, C.M., and England, P.C., Thermal regimes and regional metamorphism in the vicinity of overthrust faults: An example of shear heating and inverted metamorphic zonation from southern California, *Earth Planet. Sci. Lett., 31*, 142-152, 1976.

Graham, C.M., and R. Powell, A garnet-hornblende geothermometer: Calibration, testing, and application to the Pelona Schist, southern California, *J. Metamorph. Geol., 2*, 13-31, 1984

Jacobson, C.E., Relationship of deformation and metamorphism of the Pelona Schist to movement on the Vincent thrust, San Gabriel Mountains, southern California, *Am. J. Sci., 283*, 587-604, 1983.

Jacobson, C.E., The $^{40}Ar/^{39}Ar$ Geochronology of the Pelona Schist and Related Rocks, Southern California, *JGR, 95* (B1), 509-528, 1990.

Jacobson, C.E., Qualitative thermobarometry of inverted metamorphism in the Pelona and Rand Schists, southern California using calciferous amphibole in mafic schist, *J. Metamorph. Geol., 13*, 79-92, 1995.

Jacobson, C.E., and Dawson, M.R., Structural and metamorphic evolution of the Orocopia Schist and related rocks, sourthern California: Evidence for Late Movement on the Orocopia Fault, *Tectonics, 14,* 733-744, 1995.

Lovera, O.M., F.M. Richter, and T.M. Harrison, The $^{40}Ar/^{39}Ar$ Thermochronometry for Slowly Cooled Samples Having a Distribution of Diffusion Domain Sizes, *JGR, 94*, 17917-17935, 1989.

Lovera, O.M., M. Grove, T.M. Harrison, and M.T. Heizler, Systematic Analysis of K-feldspar Age and Kinetic Properties, *EOS, 76* (17), 287, 1995.

Mahaffie, M.J, and Dokka, R.K., Thermochronologic evidence for the age and cooling history of the upper plate of the Vincent thrust, California, , *Geol. Sci. Am. Abstr. Programs, 18*, 153, 1986.

May, D.J., and Walker, N.W., Late Cretaceous juxtaposition of metamorphic terranes in the southeastern San Gabriel Mountains, California, *Geol. Sci. Am. Bull. 101*, 1246-1267, 1989.

Miller, F.K., and D.M. Morton, Potassium-argon geochronology of the eastern Transverse Ranges and the southern Mojave Desert, southern California, *U.S. Geol. Surv. Prof. Pap., 1152*, 30 pp, 1980.

Molnar P., and England, P., Temperatures, heat flux, and frictional stress near major thrust faults, *J. Geophys. Res., 95*, 4833-4856, 1990.

Peacock, S.M., Creation and preservation of subduction-related inverted metamorphic gradients, *J. Geophys. Res., 92*, 12763-12781, 1987.

Peacock, S.M., Blueschist-facies metamorphism, shear heating, and P-T-t paths in subduction shear zones, *J. Geophys Res, 97*, 17693-17707, 1992.

Press, W.H., B.P. Flannery, S.A. Teukolsky, and W.T. Vetterling, *Numerical Recipes:The Art of Scientific Computing*, Cambridge University Press, New York, 818p., 1988.

Richter, F.M., O.M. Lovera, T.M. Harrison, and P. Copeland, Tibetan tectonics from $^{40}Ar/^{39}Ar$ analysis of a single K-feldspar sample, *Earth Planet. Sci. Lett., 105*, 266-278, 1991.

M. Grove and O.M. Lovera, Department of Earth and Space Sciences, Uviversity of California, Los Angeles, Los Angeles, CA 90024.